Journal of Biomedical Optics

SPIEDigitalLibrary.org/jbo

Photoacoustic-guided ultrasound therapy with a dual-mode ultrasound array

Amaury Prost
Arik Funke
Mickaël Tanter
Jean-François Aubry
Emmanuel Bossy

SPIE

Photoacoustic-guided ultrasound therapy with a dual-mode ultrasound array

Amaury Prost, Arik Funke, Mickaël Tanter, Jean-François Aubry, and Emmanuel Bossy
Institut Langevin, ESPCI ParisTech, CNRS UMR 7587, INSERM ERL U979, 10 rue Vauquelin, 75231 Paris Cedex 05, France

Abstract. Photoacoustics has recently been proposed as a potential method to guide and/or monitor therapy based on high-intensity focused ultrasound (HIFU). We experimentally demonstrate the creation of a HIFU lesion at the location of an optical absorber, by use of photoacoustic signals emitted by the absorber detected on a dual mode transducer array. To do so, a dedicated ultrasound array intended to both detect photoacoustic waves and emit HIFU with the same elements was used. Such a dual-mode array provides automatically coregistered reference frames for photoacoustic detection and HIFU emission, a highly desired feature for methods involving guidance or monitoring of HIFU by use of photoacoustics. The prototype is first characterized in terms of both photoacoustic and HIFU performances. The probe is then used to perform an idealized scenario of photoacoustic-guided therapy, where photoacoustic signals generated by an absorbing thread embedded in a piece of chicken breast are used to automatically refocus a HIFU beam with a time-reversal mirror and necrose the tissue at the location of the absorber. [DOI: 10.1117/1.JBO.17.6.061205]

Keywords: photoacoustics; high-intensity focused ultrasound; HIFU; HIFU monitoring; HIFU guidance; array transducer; time-reversal.

Paper 11469SS received Aug. 31, 2011; revised manuscript received Nov. 9, 2011; accepted for publication Dec. 12, 2011; published online May 7, 2012.

1 Introduction

Ultrasound waves generated by a transducer outside an organ can be brought to a tight focus deep within tissue. If the acoustic intensity is sufficiently high, viscous absorption of the acoustic waves can cause significant local heating of the tissue at the focus, while leaving tissue in the propagation path of the ultrasound unaffected. High-intensity focused ultrasound (HIFU) therefore provides the ability to cause selective tissue necrosis and is rapidly emerging as one of the most promising noninvasive treatment modalities in several medical fields, including oncology and urology.[1–3] However, the reliability and efficacy of HIFU treatments in a clinical context depends on the ability to guide and monitor in real time the deposition of acoustic energy in space (location of the heated zone) and time (amount of energy deposited), in order to control for actual tissue destruction as well as to ensure that only the targeted tissue is affected during the procedure.

To date, the latest advances in techniques developed to tackle the issue of real-time guidance and monitoring of HIFU treatments involve techniques based on magnetic resonance imaging (MRI) or ultrasound. It has been demonstrated that MRI can be used in real time to provide temperature maps and track tissue motion simultaneously,[4] but it remains limited by its cost and clinical accessibility. As an alternative, ultrasound-based techniques are also being developed to guide and monitor HIFU: Speckle-tracking techniques are used for real-time estimation and compensation of tissue motion,[5] for temperature monitoring,[6] and for measurement of changes in shear elasticity.[7]

Recently, photoacoustics has been proposed as an alternative or complementary way to either monitor[8–12] or guide[13] HIFU. Photoacoustic imaging or sensing relies on the detection of ultrasound waves generated by optical absorption via the thermoelastic effect.[14,15] Photoacoustic imaging provides information on tissue optical properties with ultrasonic resolution, at depths from subsurface up to several centimeters in biological tissue. It is therefore a potential candidate to monitor HIFU lesions, as the optical properties of tissue change during heating, and was investigated in the context of HIFU monitoring in several studies.[8–10,12] The photoacoustic effect has also been proposed as a means to guide focusing[16] based on time reversal or phase conjugation, in particular in the context of HIFU.[13] One of the main interests in using photoacoustics for monitoring and/or guiding HIFU relies on the fact that the same transducer may be used for HIFU emission and photoacoustic sensing, providing automatically coregistered reference frames for photoacoustic detection and HIFU emission. The focusing method based on photoacoustic detection presented by Bossy and Daoudy et al.[16] and discussed in the context of HIFU guidance by Funke and Aubry et al.[13] inherently relies on the use of the same transducer array for both photoacoustic detection and ultrasound emission. In Funke and Aubry et al.,[13] a scenario of photoacoustic-guided therapy was demonstrated, but without the use of high-intensity acoustic emission. The principle of HIFU emission was illustrated by use of high-intensity ultrasound burst but limited to a few hundred microseconds in length, due to the impossibility of the imaging probe to sustain power emission for seconds-long duration, as required for ultrasound therapy. Refocusing was performed in a water tank, with no tissue sample and no HIFU lesion.

In the current paper, we experimentally demonstrate the creation of a HIFU lesion at the location of an optical absorber, by use of a dual-mode ultrasound array prototype that was used for both HIFU emission and detection of photoacoustic signals emitted by the absorber. In published works involving both

Address all correspondence to: Emmanuel Bossy, Institut Langevin, ESPCI ParisTech, 10 rue Vauquelin, 75231 Paris Cedex 05, France. Tel: +33140794590; Fax: +33140794537; E-mail: emmanuel.bossy@espci.fr.

0091-3286/2012/$25.00 © 2012 SPIE

HIFU emission and photoacoustic detection, either two different transducers were used for each modality[13] or a single-element focused transducer was used.[10,11] The use of the same array transducer for both photoacoustic detection and HIFU emission is the only way to benefit from the flexibility of ultrasonic dynamic focusing and imaging, and is inherently required to perform HIFU guidance.[13] In this work, we first experimentally characterize a dual-mode 128-element array prototype, both in terms of photoacoustic detection and HIFU emission. The array is then used in the context of HIFU guidance to demonstrate the formation of a HIFU lesion in a piece of chicken breast *in vitro*, based on guidance by the photoacoustic waves emitted by an optical absorber embedded in the sample.

2 Materials and Methods

2.1 *Experimental Setup*

A schematic of the experimental setup is shown on Fig. 1. The various components of this setup are described in detail in the following paragraphs.

2.1.1 *Dual-mode transducer*

The 128-element linear array was manufactured by Imasonic, France. The array has a nominal central frequency of 1.7 MHz and was designed with the following geometrical characteristics: The array is cylindrically prefocused in the elevation direction (see Fig. 2), with a focal length of 64 mm and element height of 20 mm. The array aperture is 89.6 mm. These characteristics were chosen with the expectation to both provide sensitivity for photoacoustic detection and allow the emission of HIFU. The performances of the probe are described in the results section. The transducer was provided by the manufacturer without impedance matching, with a −6 dB bandwidth (measured in pulse-echo mode) of 45% and an electrical impedance of approximately 30-j350 Ω at 1.7 MHz. The probe was impedance matched in the laboratory by use of 128 identical passive inductors ($L = 47$ μH), in order to compensate in transmission mode for the imaginary part of the electrical impedance around the central frequency, and to allow efficient power transmission to the probe for the HIFU mode. The probe was always connected to its matching box, whether the probe was used for HIFU emission or photoacoustic detection. To monitor the temperature elevation in the probe during HIFU emission, a 80-μm-diameter type-T (copper-constantan) thermocouple was embedded by the manufacturer close to the central element of the probe.

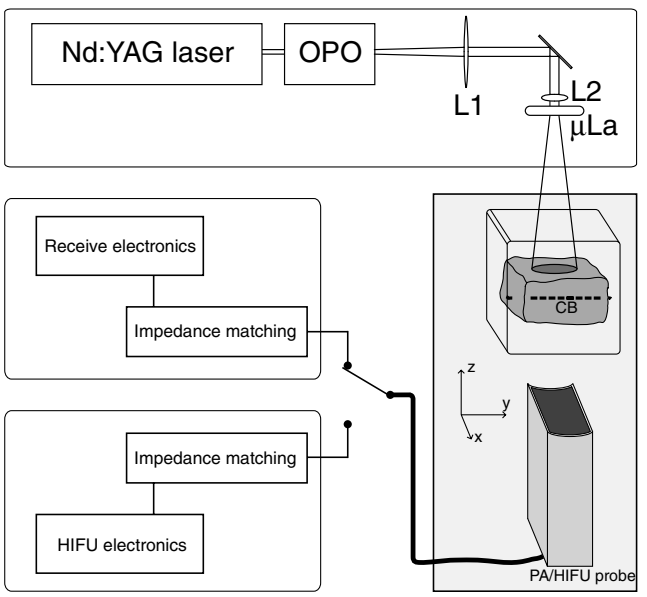

Fig. 1 Schematic of the experimental setup. L1 and L2: converging lenses; μLA: microlens array; CB: chicken breast sample.

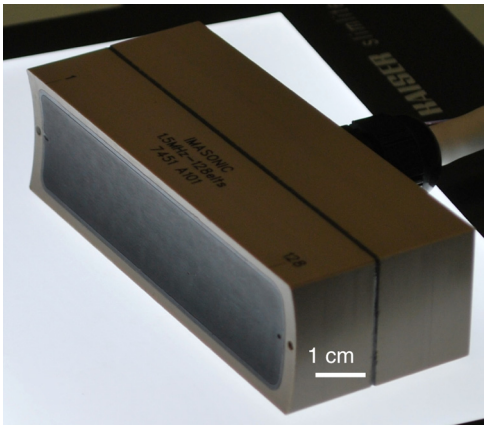

Fig. 2 Photograph of the dual-mode 128-element array prototype.

2.1.2 *Electronics*

The dual-mode prototype is intended to be used eventually on a unique multichannel electronics allowing both HIFU emission and weak ultrasonic signals detection. However, such a device was not available at the time of this work, and the probe was tested on two different multichannel systems, one for the photoacoustic detection and one for the HIFU emission. A new electronics is under development that would combine both capabilities within the same device. For photoacoustic detection, the probe was connected to a 128-channel electronics (Open system, Lecoeur Electronique, Chuelles, France), synchronized with the laser system via a digital-delay generator (BNC 505, Berkeley Nucleonics, San Rafael, CA, USA). The Open system has a receive gain tunable from 0 to 79 dB. For HIFU emission, the array was connected to a laboratory HIFU electronics (used in Ref. 13, not available commercially), with 300 fully programmable and independent channels.

2.1.3 *Optics*

The photoacoustic experiments were performed with a five-nanosecond laser pulse obtained from an optical parametric oscillator (Surelite OPO Plus, Continuum, Santa Clara, CA, USA) pumped by a frequency-doubled Nd:YAG laser operating with a repetition rate of 10 Hz (Surelite II, Continuum, Santa Clara, CA, USA). The diverging output beam was collimated by use of a converging lens to $f_{L_1} = +500$ mm obtain a beam with a diameter of the order of 20 mm. This beam was directed toward a second converging lens $f_{L_2} = +400$ mm pressed against a microlens array (circular array, EDC-10, RPC Photonics, Rochester, NY, USA) in order to provide a circular top-hat distribution of light with a diameter of 30 mm in the focal plane of the converging lens. In this plane, the maximum fluence that the laser could provide was

8 mJ · cm^{-2}. The wavelength in this study was kept constant at $\lambda = 700$ nm.

2.2 *Transducer Characterization*

All the experiments were done in a water tank. Several types of experiments were performed to characterize the performances of the probe.

2.2.1 *Photoacoustic detection*

Probe sensitivity. The detection sensitivity was assessed by direct laser illumination of the probe surface, Due to the strong optical absorption of the black layer's in front of the probe, it was assumed that the photoacoustic signal generated superficially within the layer external interface could be considered to have a bandwidth much larger than the bandwidth of the probe. Under this assumption, the signal generated by the absorption of the 5-ns laser pulse provides a direct measurement of the probe's impulse response, which was Fourier transformed to obtain the relative frequency-dependent detection sensitivity of the probe. In order to scale the frequency response of the probe with absolute sensitivity, expressed in V/MPa, the absolute sensitivity of the probe at one chosen frequency was measured with the following procedure: The tip of a steel needle (radius of curvature on the order of a few hundred microns), aligned along the z-direction, was placed 64 mm away from the probe (at its fixed elevation focal distance), in front of the central elements. A calibrated hydrophone (HGL-0200, Onda Corporation, Sunnyvale, CA, USA) was placed a few millimeters above the central elements of the ultrasound array, facing the needle tip. A 1-MHz single-element focused transducer was used to sonicate the needle tip with a 1.30-MHz continuous ultrasound wave. The frequency of 1.30 MHz was chosen to accommodate for the emission bandwidth of the 1-MHz transducer and the detection bandwidth of the array. This calibration at one frequency, combined with the measurement of the frequency-dependent sensitivity, provides a full calibration at all frequencies. The ultrasound wave scattered by the needle tip was recorded simultaneously on both the hydrophone and the central elements closest to the hydrophone. Assuming the wave detected by the hydrophone is the same as that detected by the neighboring probe elements (which was verified by replacing the array with the hydrophone), this procedure thus allowed us to calibrate the sensitivity of the probe in terms of voltage per pressure amplitude of a wave originating from the elevation focal zone (see Fig. 3).

Point-spread function. The photoacoustic spatial resolution was estimated by imaging a thin, dark hair placed 64 mm away from the probe, perpendicular to the imaging plane. The laser beam directly illuminated the hair in water. A standard delay-and-sum algorithm was used to reconstruct a photoacoustic image of the dark hair, yielding the nominal photoacoustic point spread function (PSF) of the probe. The diameter of the humain hair used was approximately 100 microns, much smaller than the measured PSF.

2.2.2 *Emission of high-intensity focused ultrasound*

For all HIFU experiments, the transducer was immersed in a tank filled with filtered and degassed water, at a temperature of 23°C. To test the HIFU capabilities of the transducer, ultrasound

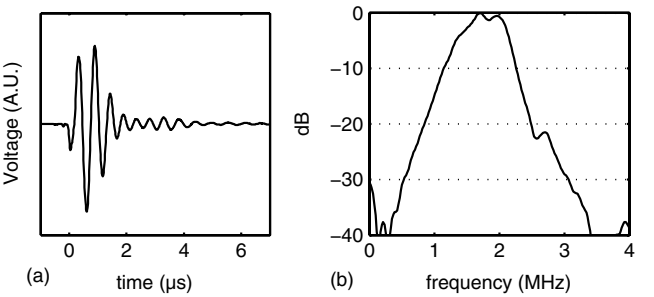

Fig. 3 (a) Temporal impulse response in receive mode. (b) Corresponding frequency response. The absolute maximum sensitivity peaks at 40 V/MPa (before amplification).

was focused electronically at the depth defined by the geometric elevation focus (64 mm), where the acoustic intensity is as high as possible. A calibrated HIFU hydrophone (HNA-0400, Onda Corporation, Sunnyvale, CA, USA) was placed at the ultrasound focus with micropositioning stages and used to measure pressure waveforms under various conditions, described below. As the hydrophone sensitivity was significantly frequency dependent in the relevant range, the following steps were carried out to obtain pressure waveforms: The highly nonlinear voltage waveforms measured with the hydrophone were first Fourier transformed. Then the spectra were converted into absolute pressure values in the frequency domain by use of the hydrophone frequency-domain calibration curves provided by the manufacturer. The converted spectra were finally inverse-Fourier transformed back into the time domain to provide absolute pressure waveforms. To test the HIFU emission behavior of the transducer, several experiments were conducted.

Emission bandwidth. To estimate the emission bandwidth, acoustic intensities for frequencies ranging from 1.1 to 1.7 MHz were computed from absolute pressure waveforms measured at focus in water by use of the following formula:

$$I = \frac{1}{\rho_0 c_0} \times \frac{1}{T} \int_0^T p^2(t) \mathrm{d}t. \quad (1)$$

Equation (1) is only approximate for strongly nonlinear fields,[17] but is intended here to provide orders of magnitude and to allow direct comparisons with the numerous publications using this formula with similar HIFU fields. For all frequencies, the driving command passed to the electronics was kept at a constant value, corresponding to the nominal value used for the photoacoustic-guided HIFU experiment described in the next section.

Temperature rise. The ability of the probe to sustain HIFU emission is closely related to the temperature increase of the probe elements. During HIFU experiments with seconds long bursts, the probe temperature was monitored in real-time with a PC-base temperature logging package (TC-08, Pico Technology, UK) connected to the thermocouple embedded in the probe. The probe was designed to sustain temperature increase up to at least 60°C, according to the manufacturer.

2.3 *Photoacoustic-Guided Ultrasound Therapy*

For the proof-of-concept 'photoacoustic-guided HIFU' scenario, a black thread 0.5 mm in diameter was inserted along the y-axis (across the imaging plane, see Fig. 1) in the middle

of a 3-cm-thick slab of chicken breast. The chicken breast was embedded in a block of agar gel (1.5% in mass) of dimensions $7 \times 7 \times 5$ cm^3. The chicken breast was illuminated with 700-nm laser pulses with an energy on the order of 50 mJ spread over a circular area 30 mm in diameter, corresponding to a fluence of about 8 mJ $\cdot$ cm^{-2}. Photoacoustic signals were recorded on the array with a single laser shot and a receive gain of 60 dB.

The photoacoustic signals were then used as in Ref. 13 to automatically guide HIFU toward the black thread. Briefly, the photoacoustic signals were time reversed to achieve automatic refocusing toward the optical absorbers (see Refs. 13 and 16 for further details). We then extracted the frequency component of these time-reversed signals corresponding to desired HIFU frequency, in order to generate a monochromatic HIFU therapeutic beam. In this experiment, only the phase information was used, while the amplitude of each channel was set at the same value on each channel to optimize the HIFU energy delivered at focus. Note that as two different electronics were used for reception and emission, as explained earlier, a manual switch between the two electronics was performed between the photoacoustic detection and the HIFU emission. The amplitude and exposure time of the HIFU burst used to necrose the chicken breast were chosen based on the results of the probe characterization presented in Sec. 2.2. An exposure time of 10 sec and a focal intensity of about 1900 W/cm^2 ($p_+ = 15$ MPa and $p_- = -5$ MPa) were chosen to necrose the chicken while limiting the temperature rise in the probe.

3 Results

3.1 *Photoacoustic Detection*

Figure 3 shows the impulse response [Fig. 3(a)] and the corresponding frequency response [Fig. 3(b)] of the probe used in receive mode. The measured −6 dB bandwidth is 50%, with a central frequency of approximately 1.8 MHz. It was observed that this response is only very weakly affected by the matching network designed for the transmission mode (results not shown here). The peak sensitivity [0 dB on Fig. 3(b)] corresponds to an absolute sensitivity of 40 V/MPa. Note that voltage refers to the voltage measured at the probe connector while plugged onto the electronics, but before amplification. This sensitivity was found to be similar to that of conventional imaging array with comparable characteristics (frequency, compensation for element size). When the maximum gain (79 dB) is used, the corresponding highest sensitivity of the system is 340 mV/Pa. The input voltage range of the electronics is 5 V, which corresponds to a pressure range at full amplification of about 15 Pa. The electronics noise at full amplification range was measured to be approximately 5 nV/(Hz)$^{1/2}$, which turns to a noise-equivalent pressure of 0.25 Pa in a 4-MHz frequency bandwidth (that includes the reception bandwidth of our prototype). These numbers are of course relevant for spherical pressure waves emitted from the focal region (elevation focus) of the transducer.

Figure 4 shows the photoacoustic PSF derived from the photoacoustic emission from the dark hair, using the full aperture of the probe and no apodization. The −6 dB focal region (white contour) has a transverse dimension of 1.1 mm and an axial dimension of 1.5 mm.

3.2 *Emission of High-Intensity Focused Ultrasound*

Figure 5(a) plots the acoustic intensity measured in water with the hydrophone at focus as a function of frequency. It illustrates the frequency-resonant impedance matching produced in transmission by the passive inductors. The optimum frequency for HIFU emission turned out to be close to 1.35 MHz. Figure 5(b) plots the pressure waveform measured in water at focus at the optimum frequency of 1.35 MHz. The peak pressure values are $p_+ = 15$ MPa and $p_- = -5$ MPa, corresponding to an acoustic intensity on the order of 1900 kW/cm^2, derived from Eq. (1).

Figure 6 illustrates the temperature increase measured with the thermocouple, for a 10-sec HIFU emission corresponding to the pressure waveform plotted on Fig. 5(b). The probe was immersed in a large 23°C water tank, with no water circulation. The observed maximum probe temperature under these conditions was approximately 43°C, well below the prescribed maximum temperature of 60°C (see Sec. 2.2).

3.3 *Photoacoustic-Guided Ultrasound Therapy*

Figure 7 is the final result of this work. It shows a lesion obtained by targeting a black thread, as described in the materials and methods section. The focusing of high-intensity ultrasound was based on the time reversal of the 1.35-MHz component of the photoacoustic signals produced by the illumination of the black thread. On Fig. 7, the illumination comes from the bottom, and the HIFU beam comes from above the sample. Although not shown here, lesions could be obtained under various conditions (different exposure durations and amplitudes).

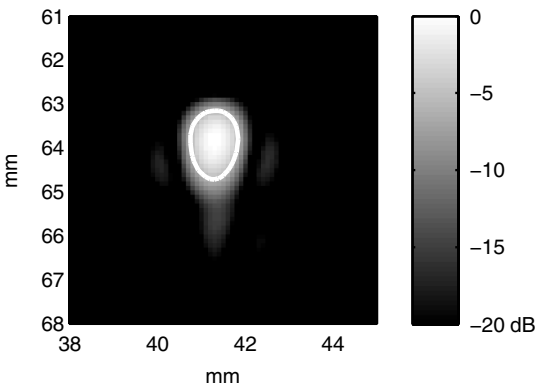

Fig. 4 Photoacoustic point spread function, measured with a thin, dark hair as the optical absorber. The white contour indicates the 6-dB focal region.

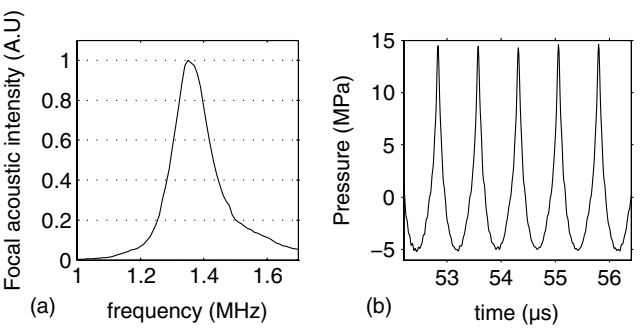

Fig. 5 (a) Normalized focal acoustic intensity as a function of frequency, for a fixed drive command. (b) Corresponding focal waveform measured at $f = 1.35$ MHz.

The lesion shown on Fig. 7 was obtained with 10 sec of exposure and a focal intensity of about 1900 W/cm^2, but lesions were also obtained with a longer burst of 20 or 30 sec and lower acoustic intensities. The conditions used here were used to demonstrate that even for a relatively rapid heating of 10 sec in duration, the temperature increase in the probe was low enough. Moreover, active cooling (for instance using flowing cold water at the surface of the probe) could be used if temperature rise became a problem, as might happen if continuous HIFU emission was required.

4 Discussion and Conclusion

In this work, a transducer array was used for both photoacoustic detection and ultrasound therapy. While the idea of using photoacoustic signals to guide HIFU beams has been introduced in earlier works,[13,16] it is the first time to our knowledge that a dual-mode array has been used to demonstrate experimentally photoacoustic-guided ultrasound therapy with a commercially available transducer technology. In homogeneous acoustic media, the array can provide photoacoustic images automatically coregistered with the HIFU lesion, a highly desired feature for monitoring of the photoacoustic changes at the lesion location. In the case of complex and/or aberrating media where imaging is not possible, the ability to focus therapeutic ultrasound is equivalent with our dual-mode array to the ability to selectively detect the photoacoustic signals emitted from the targeted region. Therefore, methods developed to guide HIFU beams based on photoacoustic signals should also prove valuable to perform photoacoustic-based monitoring of HIFU lesions.

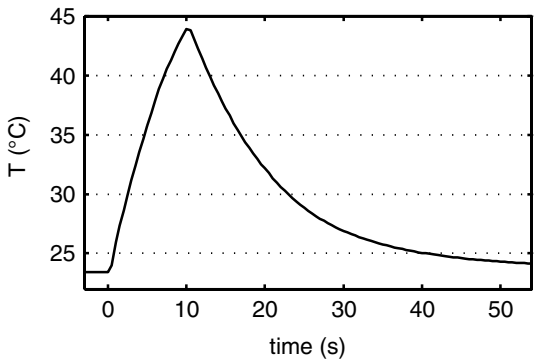

Fig. 6 Temperature in the probe for a 10-sec HIFU emission ($I = 1900$ kW/cm^2).

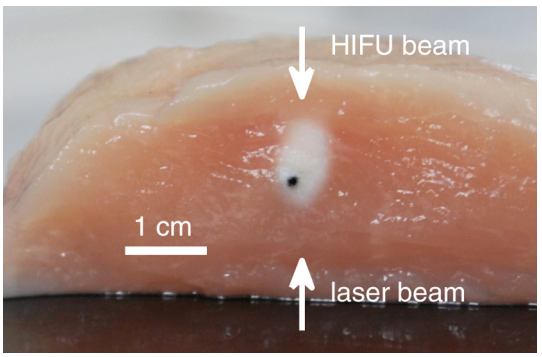

Fig. 7 Lesion obtained *in vitro* in chicken breast by focusing HIFU based on the photoacoustic signals emitted by the optical absorber.

Several ideal conditions were chosen to perform our proof-of-concept experiment. In particular, a single and strong optical absorber was used to generate the photoacoustic signals, at a rather small optical depth in the sample (about 15 mm). These conditions were chosen to allow straightforward refocusing by time reversing the photoacoustic signals at a single frequency. This approach assumes that the photoacoustic signals were emitted from a single location, and also requires a fairly good signal-to-noise ratio (SNR). Our system was also demonstrated to detect photoacoustic signals from a dark thread embedded at several centimeters in chicken breast (results not shown here), in agreement with results already published in the literature.[18,19] However, for absorbers located centimeters deep in tissue, the much weaker SNR requires the development of efficient algorithms making use of the information available at all frequencies, as opposed to the approach performed in this work where only a single frequency was used. We are currently investigating an optimized algorithm to focus HIFU bursts based on noisy broadband signals. In the situation presented in this work, where no acoustically complex and/or aberrating medium was involved, the easiest approach would have been to build a photoacoustic image of the medium, and then to identify the location of the HIFU target on the photoacoustic image. However, such an approach would fail in the presence of acoustically more complex media. Moreover, when real time is needed, for instance to perform HIFU therapy in presence of tissue motion, an automatic focusing method is required. Therefore, although we demonstrated the use of our probe in the case of a homogeneous acoustic medium, the approach used is in fact more general and appropriate even in situations where no photoacoustic images can be obtained. At the time of this work, a single electronics for both photoacoustic detection and HIFU emission was not available. Switching between the two electronics used in this study made real time impossible. However, with the upcoming single electronics, real-time tracking and processing of the photoacoustic signals should be readily available. One important challenge that was not undertaken here deals with the necessity of selectively and automatically detecting the targeted optical absorber even when it is embedded in a medium with significant photoacoustic background, such as expected in biological tissue *in vivo*. In an earlier work,[13] we demonstrated that it is possible to detect selectively a photoacoustic contrast agent embedded in a medium with strong photoacoustic background based on the wavelength dependence of the contrast agent. But this demonstration was done with a basic tissue-mimicking phantom. Performing photoacoustic-guided ultrasound therapy *in vivo* therefore requires further work to solve the challenges of selective detection in realistic conditions and efficient automatic refocusing in low-SNR conditions.

In conclusion, we characterized a dual-mode 128-element ultrasound array designed for both photoacoustic detection and ultrasound therapy. The array was used to demonstrate the automatic focusing of a HIFU beam toward an optical absorber, based on the photoacoustic waves emitted by the absorber. Although this proof of concept was performed in optimal conditions, in the context of HIFU guidance, these results pave the way for further developments of photoacoustic-assisted ultrasound therapy, for both guidance and monitoring.

Acknowledgments

The authors would like to acknowledge Romain Bollart for his help with characterizing the probe. This work was supported by the Agence Nationale de la Recherche (ANR grant PAG-HIFU JCJC07-195015).

References

1. F. Wu et al., "Extracorporeal focused ultrasound surgery for treatment of human solid carcinomas: early Chinese clinical experience," *Ultrasound Med. Biol.* **30**(2), 245–260 (2004).
2. J. E. Kennedy, "High-intensity focused ultrasound in the treatment of solid tumours," *Nat. Rev. Cancer* **5**(4), 321–327 (2005).
3. R. O. Illing et al., "The safety and feasibility of extracorporeal high-intensity focused ultrasound (HIFU) for the treatment of liver and kidney tumours in a Western population," *Br. J. Cancer* **93**(8), 890–895 (2005).
4. C. T. W. Moonen, B. D. de Senneville, and C. Mougenot, "Real-time adaptive methods for treatment of mobile organs by MRI-controlled high-intensity focused ultrasound," *Magn. Reson. Med.* **57**(2), 319–330 (2007).
5. M. Pernot, M. Tanter, and M. Fink, "3-D real-time motion correction in high-intensity focused ultrasound therapy," *Ultrasound Med. Biol.* **30**(9), 1239–1249 (2004).
6. R. Seip and E. S. Ebbini, "Noninvasive estimation of tissue temperature response to heating fields using diagnostic ultrasound," *IEEE Trans. Biomed. Eng.* **42**(8), 828–839 (1995).
7. B. Arnal, M. Pernot, and M. Tanter, "Monitoring of thermal therapy based on shear modulus changes: I. shear wave thermometry," *IEEE Trans. Ultrason. Ferroelectrics. Freq. Contr.* **58**(2), 369–378 (2011).
8. K. V. Larin, I. V. Larina, and R. O. Esenaliev, "Monitoring of tissue coagulation during thermotherapy using optoacoustic technique," *J. Phys. D* **38**(15), 2645–2653 (2005).
9. T. D. Khokhlova et al., "Optoacoustic monitoring of HIFU therapy: feasibility study" in *Therapeutic Ultrasound Book Series: 5th International Symposium on Therapeutic Ultrasound. AIP Conf. Proc.*, October 27–29, Boston, MA, G. T. Clement, N. J. McDannold, and K. Hynynen, Eds., Vol. 829, pp. 181–185 (2006).
10. H. Z. Cui, J. Staley, and X. M. Yang, "Integration of photoacoustic imaging and high-intensity focused ultrasound," *J. Biomed. Opt.* **15**(2), 021312 (2010).
11. H. Z. Cui and X. M. Yang, "*In vivo* imaging and treatment of solid tumor using integrated photoacoustic imaging and high-intensity focused ultrasound system," *Med. Phys.* **37**(9), 4777–4781 (2010).
12. P. V. Chitnis et al., "Feasibility of optoacoustic visualization of high-intensity focused ultrasound-induced thermal lesions in live tissue," *J. Biomed. Opt.* **15**(2), 021313 (2010).
13. A. R. Funke et al., "Photoacoustic guidance of high intensity focused ultrasound with selective optical contrasts and time-reversal," *Appl. Phys. Lett.* **94**(5), 054102 (2009).
14. A. A. Oraevsky, S. L. Jacques, and F. K. Tittel, "Measurement of tissue optical properties by time-resolved detection of laser-induced transient stress," *Appl. Opt.* **36**(1), 402–415 (1997).
15. M. H. Xu and L. H. V. Wang, "Photoacoustic imaging in biomedicine," *Rev. Sci. Instrum.* **77**(4), 041101 (2006).
16. E. Bossy et al., "Time reversal of photoacoustic waves," *Appl. Phys. Lett.* **89**(18), 184108 (2006).
17. M. F. Hamilton and D. Blackstock, Nonlinear acoustics, *Acoustical Society of America*, American Institute of Physics, Melville, NY (2008).
18. R. O. Esenaliev, A. A. Karabutov, and A. A. Oraevsky, "Sensitivity of laser opto-acoustic imaging in detection of small deeply embedded tumors," *IEEE J. Sel. Top. Quant. Electron.* **5**(4), 981–988 (1999).
19. G. Ku and L. H. V. Wang, "Deeply penetrating photoacoustic tomography in biological tissues enhanced with an optical contrast agent," *Opt. Lett.* **30**(5), 507–509 (2005).